ITC 2/52
Information Technology and Control
Vol. 52 / No. 2 / 2023
pp. 322-335
DOI 10.5755/j01.itc.52.2.32796

Human Dental Age and Gender Assessment from Dental Radiographs Using Deep Convolutional Neural Network

Received 2022/11/17 | Accepted after revision 2022/12/20

HOW TO CITE: Hemalatha, B., Bhuvaneswari, P., Nataraj, M., Shanmugavadivel, G. (2023). Human Dental Age and Gender Assessment from Dental Radiographs Using Deep Convolutional Neural Network. *Information Technology and Control,* 52(2), 322-335. https://doi.org/10.5755/j01.itc.52.2.32796

Human Dental Age and Gender Assessment from Dental Radiographs Using Deep Convolutional Neural Network

B. Hemalatha
Department of Information Technology, Dr. N. G. P. Institute of Technology, Coinbatore, 641048, India

P. Bhuvaneswari
Department of Computer Science and Engineering, Sona College of Technology, Salem, 636005, Tamilnadu, India

Mahesh Nataraj
Department of Electronics and Instrumentation Engineering, Kongu Engineering College (Autonomous), Perundurai, Erode, Tamil Nadu, India

G. Shanmugavadivel
Department of Electronics and Communication Engineering, M. Kumarasamy College of Engineering, Karur-639113, Tamilnadu, India

Corresponding author: bhemalathares1@outlook.com

Human gender and age identification play a prominent role in forensics, bio-archaeology, and anthropology. Dental images provide prominent indications used for dental treatment, diagnosis of disease, and forensic investigation, like age identification. Numerous dental age identification techniques come with specific boundaries, namely minimum reliability, and accuracy. Gender identification approaches are not widely researched, whereas the effectiveness and accuracy of classification are not practical and very minimal. These major issues in the existing system are considered in the formulation of the proposed approach. Deep learning approaches can effectively rectify issues of drawbacks in other classifiers. The accuracy and performance of a classifier

are enhanced with the deep convolutional neural network. The fuzzy C-Means Clustering approach is used for segmentation, and Ant Lion Optimization is used for optimal feature score selection. The selected features are classified using a deep convolutional neural network (DCNN). The performance of the proposed technique is investigated with existing classifiers, and DCNN outperforms other classifiers. The proposed technique achieves 91.7% and 91% accuracy for the identification of gender and age, respectively.

KEYWORDS: Chronological age, gender, deep learning, classification, optimization, segmentation, DCNN.

1. Introduction

Assessment of age is an essential characteristic of an individual's biological characters are predicted, and it is distinguished from chronological age. For a human, chronological age is appropriate with calendar age. Biological or physiological age, which is connected to the process of tissue and organ development, describes the time span of an individual. Dental age is one of the most important maturity markers in people, and it is frequently used in pedodontics, orthopedic, pediatric, and orthodontic surgery. Physical anthropology and forensic science both make use of this signal [14, 8].

Estimation and assessment of age from a dental image are significant that is also necessary for the current era. The clinical procedure of identifying chronological age is critical, and it requires an effective indicator for identifying teeth. Furthermore, some approaches utilized in assessing age with orthopantomogram (OPG) images are highly time-consuming, and the observer's subjectivity highly influences the outcome of the estimation. Age identification is exploited over the best quality radiological OPG images [30]. Numerous forms of dental images are incorporated in age identification, and X-rays of dental images are processed for acquiring necessary information. The different dental images utilized in dentistry are panoramic bitewing, X-ray, and periapical X-ray.

The X-ray images can expose the buried structures of dental images, and computational techniques are incorporated in the process of identification as well as the classification of age, disease, and other necessary aspects of the dental image. In gender identification and dental age classification, computational intelligence such as machine learning, fuzzy, and optimization techniques are broadly utilized for defining a projection from a set of input data [28]. With the assistance of computational techniques, an unknown person's age is assessed by correlating it with any person's dental, physical, and skeletal maturity [33].

The noticeable fields of dental inquiries are dental treatment and forensics, where they face complications in assessing the details of an unknown individual. The eminence of dental images is inclined the uneven exposure and low contrast. This context motivated various researchers to do research on dental image classification. This situation motivates the necessitates of a segmentation process that leads to the delineation of the false contour of teeth [24]. The partitioning and pertaining approach to the dental radiographs images are initiated in a preceding couple of years. Many research articles have reported the dental image classification approaches that encompass enhancement, segmentation, and retrieval of definite shape from the dental image [6] that utilizes the image retrieval strategy [19] and morphological operations. Some of the approaches are developed in iterative and versatile thresholding [20, 21].

The issues in the traditional and existing techniques are considered in designing the proposed technique. A deep neural network (DNN) incorporates several unit layers with exceptionally optimized approaches and architectures. In this article, dental image classification is attained by Deep CNN with the rectified linear unit (ReLU) as an activation function. The deep learning technique avoids complicated abstraction and training of hierarchical depiction of information in the multi-dimensional format. The neural network is inspired by the functioning of neurons and resembles the nervous system of humans and the brain structure.

1.1. Contribution

The significant contribution of the article is:

- The deep learning technique can effectively do the classification. In the pre-processing, Histogram equalization is combined with ADF to attain better smoothing accuracy and noise removal.

- The significant geometrical features of the teeth are highlighted by the Fuzzy C-Means Clustering Process (FCM). The highlighted portion identifies the best feature score by Ant Lion Optimization (ALO) technique.
- The geometrical features are extracted in the optimal feature selection phase, enhancing the human age and gender identification process. The optimal features are classified with the assistance of a Deep Convolutional Neural Network (DCNN).

The order of the remaining text is as follows: in Section 2, different gender identity and dental age classification techniques are addressed. The suggested DCNN approach is presented in Section 3. The results of the DCNN classification are demonstrated in Section 4, and the paper is completed in Section 5.

2. Related Work

Identification and estimation of the age of an individual have a prominent role in forensic ontology. The dental images are examined for different purposes, such as diagnosis and treatment. Most researchers focused their research on disease diagnosis, and later, it was employed for age identification. The dental age is classified by the classifiers, namely Decision Tree (DT), SVM, and K-Nearest Neighbor (KNN), which uses the features retrieved by the AlexNet and ResNet-based neural network [17]. In some research work, the biological features, namely bone, dental structures, face, and skeleton, are considered while classifying dental images [5].

The Active Contour Model (ACM) with Jaya Optimization (JO) is utilized for image segmentation. The process of classification is simplified and optimized by the effective segmentation technique. The segmented image facilitates easy access, and the needed features are retrieved. The Modified Extreme Learning Machine with Sparse Representation Classification (MELM-SRC) is performed with the retrieved features, identifying the dental age [15]. The estimation of dental age is attained by the mathematical approach and Demirjian Score which uses panoramic radiographs to investigate the dental age of an individual [32].

Most of the researchers focused on identifying age, and the identification of gender has not been examined elaborately yet. The dental features are employed in age identification, whereas geometric features are utilized in gender identification. Additionally, dental images and skeleton remains are used for gender identification. The dental image is examined by the Buccolingual (BL) and Mesiodistal (MD) measurements with diverse forms of teeth and geometric features. The level of accuracy varies for every geometric feature of the dental images that is Maxillary Posterior Teeth attain 67.9% identification accuracy, and Teeth from the Jaw attain 92.5% identification accuracy [4].

The image classification requires effective pre-processing and segmentation techniques, whereas Gray Level Co-occurrence Matrix is applied for the segmentation. The needed features are retrieved and denoted in the matrix, then classified using the Random Forest (RF) technique. The process of matrix representation is complex, making the retrieval process ineffective and highly time-consuming [3]. The feature selection process is accomplished by Discrete Cosine Transform (DCT), and the significant retrieved features are classified by RF technique.

The DCT-based RF classification technique utilizes three-dimensional tooth plaster models and a limited number of samples used for the classification. The DCT necessitated quantization, making the process complicated when the data size is enormous [12]. The cone-beam computed tomography (CBCT) images are used, and a hybrid Genetic Algorithm (GA) based Naïve Bayes (NB) approach is used for the gender classification. The features are retrieved by GA and classified by NB. The genetic algorithm fails to support the exploitation ability. GA is time-consuming and computationally expensive [1].

A completely automated method that determines gender is based on the 3D anthropometric measurements of test participants. Human posture was detected using a Kinect 3D camera, and ody measures were employed as characteristics for categorization. KNN, SVM classifiers, and neural networks were employed in conjunction with the parameters to categorize the gender. The experiment employed a unique dataset compiled from 29 female and 31 male volunteers (a total of 60 persons), and the cross-validation method was the Leave One Out methodology. The greatest accuracy for SVM using an MLP kernel function is 96.77% [11].

Various traditional machine learning and optimization techniques are employed in dental age and gender identification, which are highly time-consuming; classification is influenced by error. The accuracy is minimum in some algorithms. The age and gender assessment techniques have certain limitations and drawbacks. By considering the drawbacks, a practical deep learning-based approach is proposed to identify gender and age.

3. Proposed Deep CNN Classifier for Human Age and Gender Identification Using Dental image

This section discusses age and gender identification with the deep learning technique, where the automatic identification of age and gender requires numerous image processing techniques. The significant features are identified with the assistance of an optimization algorithm and the classification is attained using a deep learning approach. Based on the feature vectors, DCNN classifies the age and predicts the age of an individual. The overall block diagram of human age and gender classification is given in Figure 1.

3.1. Image Acquisition

Image acquisition is initially made for image processing, and it is the action of extracting the image from the relevant source. The acquired dental images are transmitted to the pre-processing phase.

3.2. Pre-Processing – Histogram Equalisation with Anisotropic Diffusion Filter (ADF)

ADF is used during the pre-processing to improve smoothing accuracy and noise reduction. ADF uses a selective diffusion technique based on a probabilistic characterization of the dental picture. In the diffusion zones, it reduces presumably acceptable information (i.e. regions and for diagnosis). It is still possible to see where unwanted noise has been eliminated from important structures and irrelevant parts. The primary intent of the ADF filter is to minimize noise and highly preserve the edge information [31]. The image degradation by the ADF is prevented by the image enhancement approach done by the Histogram equalization. It alters the intensities of the image, which enhances the contrast of the image [26].

Figure 1
Overall Methodology of Human Age and Gender Classification

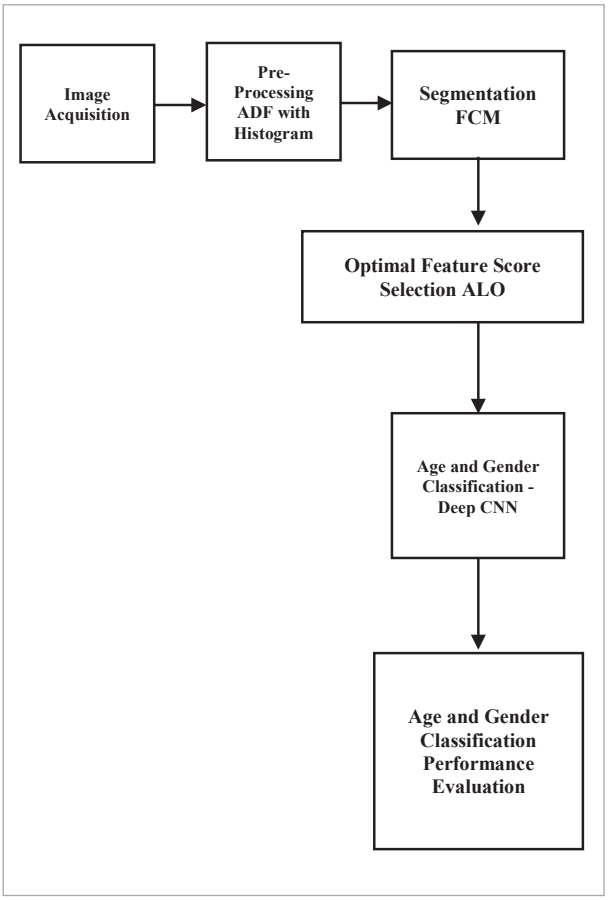

3.3. Image Segmentation and Optimal Feature Score Selection

The significant geometrical features of the teeth are highlighted by the Fuzzy C-Means Clustering Process (FCM) [9]. The fuzzy membership function is assigned with pixel value by the FCM technique. Let the IM=(im_1, im_2,.....,im_n) denote a dental image with N number of pixels partitioned into cls of clusters where mi denotes the image feature. This approach is optimized iteratively, which reduces the cost function.

$$CF = \sum_{j=1}^{N}\sum_{i-1}^{cls} mp_{ij}^{con1} \left\| im_j - cc_i^{\,2} \right\|, \quad (1)$$

where mp_{ij}indicates the membership pixel value im_j in the i^{th} cluster, cc_i is the i^{th} cluster's center position,

the norm metric value is indicated by || ||, and the constant value is indicated by con1. The con1 controls the partitioned fuzzy values.

The cost function is reduced when the pixels reside close to the cluster's centroid and are allocated with a high membership value. The pixels away from the centroid are allocated with minimum membership value. The probability of pixel is indicated by the membership function of a distinct cluster. This probability relies on the distance between the pixel and every center position of an individual feature. The cluster centers and membership function is updated as follows:

$$mp_{ij} = \frac{1}{\sum_{k=1}^{cls}\left(\frac{\left\|im_j - cc_i\right\|}{\left\|im_j - cc_k\right\|}\right)^{2/(con1-1)}} \quad (2)$$

and

$$cc_i = \frac{\sum_{j=1}^{N} mp_{ij}^{con1} im_j}{\sum_{j=1}^{N} mp_{ij}^{con1}}. \quad (3)$$

The process is initiated with every center position of the cluster. The convergence of FCM generates a solution for cc_i to denote the saddle point or local minimum value of the cost function. The convergence incidence is identified by comparing alterations in the center of the cluster or membership function at successive iterations. The neighboring pixels may hold similar or greater feature values. Identification of correlation among this cluster is significant, and this is equated as the following:

$$pb_{ij} = \sum_{k \in NB(im_j)} mp_{jk}, \quad (4)$$

where the squared window centered on the pixel (im_j) in the spatial domain is indicated as NB(im_j). The probability of the cluster in the spatial domain is indicated as pb_{ij} of the pixel im_j in cluster i. The membership function of the spatial function is given as follows:

$$mp_{ij}^{t} = \frac{mp_{ij}^{p} pb_{ij}^{q}}{\sum_{k=1}^{cls} mp_{kj}^{p} pb_{kj}^{q}}, \quad (5)$$

where the relative significance of the cost function is indicated as p and q. The pixel with high noise is minimized by this formula and labels with a neighbor pixel value. This approach corrects wrongly segmented pixels. The segmented image is passed to the optimal feature selection phase.

The geometrical features are retrieved in the optimal feature selection phase that helps in age and gender identification. The optimal features are classified with the Ant Lion Optimization technique (ALO) [22]. The best solution across the iterations is maintained by incorporating elitism. The process is guided by the random walk of an ant, which is selected by the elite antlion and antlion. The repositioning of these pixels is accomplished by the average of random walks by

$$Ant_i^t = \frac{RW_{AL}^t + RW_{EAL}^t}{2}, \quad (6)$$

where RW_{AL}^t that indicates the roulette wheel selects the antlion, and RW_{EAL}^t indicates elite ant lion.The ALO process is illustrated in Algorithm 1.

Algorithm 1. The ALO process

Input: Dental Images

Output: Optimal Feature Scores

Set the initial ant and antlion population at random

Estimation of fitness function

Identification of effective antlions and adopt it as the best optimums

while the end criterion is not satisfied

for every ant

Choose an antlion utilising Roulette wheel

Update

Create a random walk and normalize

Update the position of ant

end for

Estimate the fitness of all ants

Replace an antlion with its relevant ant it if becomes fitter

Update elite if an antlion becomes fitter than the elite

end while

Return elite

3.4. Classification – Deep Convolutional Neural Network (DCNN)

Using the aid of a Deep Convolutional Neural Network with Rectified Linear Unit (ReLu) as an activation function, the best characteristics are categorized [35]. The feature extraction and classification phases make up DCNN. Convolution and pooling layers compose the feature learning step. The fully connected and softmax layer are present during the classification step. Learning about visual features is made easier by Deep CNN, and categorization is straightforward. Figure 2 shows the Deep CNN architecture.

Figure 2
Outline of Deep CNN with RELU

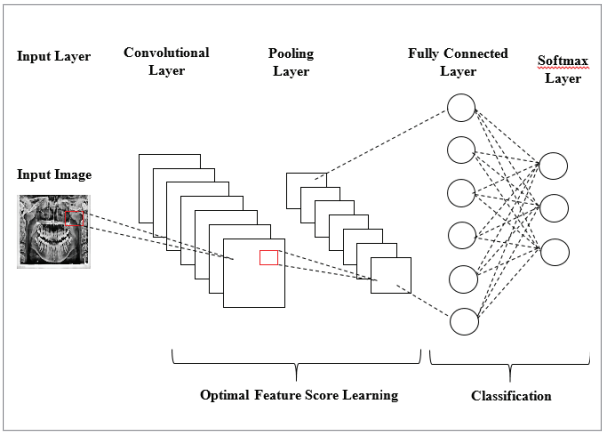

Convolution Layer

This layer has several filters that glide over the input data, and the summing is calculated by multiplying the elements one by one. The output value of this layer is therefore judged to be the input's receptive rate. The weighted summation value is regarded as one of the input elements for the layer below. The focus region is a slide that fills in the values of the other pixels in the convolutional layer's output. Zero padding, stride, and filter size are provided for each operation in the convolution layer.

The Rectified Linear Unit (ReLU) serves as an activation function that quickens the stochastic descent gradient's convergence. The value of the activation function is transferred to zero in thresholding, making ReLU implementation simple and effective. If the value is negative, it returns zero, and if the value is positive, it returns t. ReLU is provided as the following:

$$AF = \max \max\left(0, t\right). \tag{7}$$

The gradient method stops learning when the AF value reaches zero, and the leaky ReLU is activated in that case. Its function is given as follows:

$$AF_l = \begin{cases} tt > 0 \\ o \times tt \le 0 \end{cases}, o, \tag{8}$$

where the predefined parameter is indicated as o and assigned with the value 0.01

Pooling Layer

The pooling layer minimizes the output dimension, and the most familiar max-pooling technique indicates the maximum pooling filter value. The max-pooling is the most promising approach and gives significant downsampling input size. The Max pooling technique is better than the summation and averaging method.

Fully Connected Layer

This layer combines the non-linear data of the high-range characteristics that the convolutional layer's output indicates. The non-linear function in that space is learned by this layer.

Softmax Layer

This layer carries out the classification, and the output layer makes use of the softmax function, which is regarded as a normalized exponent value of output data. This shows that the output function and probability are distinct. Further, the exponential pixel value increases the probability to the maximum level. The softmax is equated as the following:

$$Op_x \frac{e^{z_x}}{\sum_{x=1}^{M} e^{z_x}}. \tag{9}$$

The output count x for the softmax output is denoted as opx, the output counts x before the softmax is denoted as zx, and the total output node count is denoted as M. In this layer, the class labels are categorized.

4. Result and Discussion

This section analyses and investigates the effectiveness of the DCNN-based categorization of a person's dental gender and age using the currently available different classifiers, including Random Forest (RF) [25], Naive Bayes (NB) [34], Convolutional Neural Network (CNN) [27], and Support Vector Machine (SVM) [31]. The dataset primarily includes OPG pictures that are used for training and testing. MATLAB analyses the simulation outcome, and the trained image size is 275 × 158 pixels. The proposed approach is trained by 60% of the total image, and 40% is used for testing. The age values are assigned as values in the hidden nodes based on the features, the relevant values are mapped with the corresponding age node.

4.1. Dataset Description

The Ortho Pantomo Gram (OPG) dataset is gathered from the Kovai Scan Center, Coimbatore. The OPG images of hundred healthy Indian Juveniles and children of age 4-18 are employed in investigating the gender and dental age, which is then compared with the chronological information of the individual. The different numbers of images are used for training and testing. The performance metrics are compared for diverse counts of images.

4.2. Performance Metrics

The effectiveness of the new method DCNN is evaluated in comparison to the current methods of Random Forest (RF), Naive Bayes (NB), Convolutional Neural Network (CNN), and Support Vector Machine (SVM) [25, 34, 30, 2]. Accuracy, Sensitivity, and Specificity are the performance criteria used to examine these techniques [13, 18, 10].

4.2.1. Accuracy

The number of correctly identified age and gender occurrences divided by the total number of instances provides an approximation of the classification accuracy of the dental picture. The classification model's effectiveness is determined by the accuracy value. The true positive (TP) and real negative (TN) values produced by the age and gender classes are used to gauge accuracy. The algorithm with maximum accuracy is termed an effective classification algorithm. The accuracy value is estimated as follows:

$$Accuracy = \frac{True\ Positive\ (TP) + True\ Negative\ (TN)}{True\ Positive\ (TP) + True\ Negative\ (TN) + False\ Positive\ (FP) + False\ Negative\ (FN)} \quad (10)$$

4.2.2. Sensitivity

Sensitivity is expressed as the rate of TP and refers to the proportion of positive or properly categorized values among all instances. It indicates the values that were correctly identified after the test, where higher sensitivity will result in lower specificity rates and vice versa. The performance of proper identification is determined by the TP value, and the evaluation of sensitivity is provided as follows:

$$Sensitivity = \frac{TP}{TP + FN}. \quad (11)$$

4.2.3. Specificity

Specificity, often known as the rate of TN, is defined as the proportion of negative or erroneously categorized values among all the cases. The assessment of specificity is provided as follows, and it aids in the identification of correctness across the entire classification sample:

$$Specificity = \frac{TN}{TN + FP}. \quad (12)$$

When the rate of TP value increases, the rate of TN values will decrease, leading to the existence of a trade-off among various classification thresholds, the trade-off among the value is depicted by Receiving Operating Characteristic Curve (ROC) [23].

4.3. Performance Evaluation

The classification performance of the DCNN is compared with the existing technique, the pre-processing technique enhances the image, and the needed features are retrieved by the process of segmentation and feature selection. The retrieved information is transmitted to the classification phase. The batch size is 128 with Stochastic Gradient Descent with momentum optimizer where the learning rate is 0.016 and drop factor is 0.1. It utilizes 8 channels at the batch normalized layer and 29 classes at the fully connected

layer. The features, their relevant age, and gender are stored in the layers.

4.3.1. Pre-Processing

Histogram Equalization (HE) and Anisotropic Diffusion Filter (ADF) are used in this study to pre-process the images. Figure 3 displays the results of the image's pre-processing

Figure 3
Input Image and Pre-Processed Image

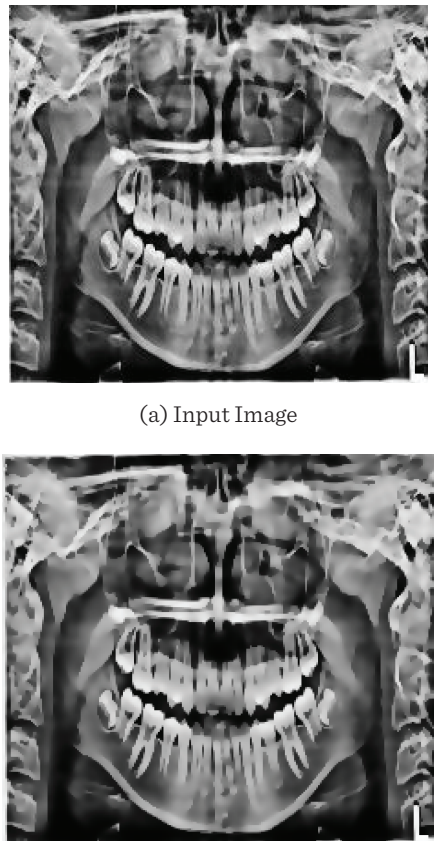

(a) Input Image

(b) ADF with HE

The input picture is shown in Figure 3(a), and the pre-processed image is shown in Figure 3(b). ADF completes the pre-processing with EQ, greatly preserving the edge information and removing the noise value. The histogram equalization keeps the image quality from deteriorating. Figure 3 shows the pre-processed and improved picture (b).

4.3.2. Segmentation – Fuzzy C-Means Clustering (FCM)

The process of segmentation alters the image illustration, which makes image analysis simple and more accessible. The FCM technique accomplishes the segmentation, and it is given in Figure 4.

Figure 4
Segmented Image – FCM

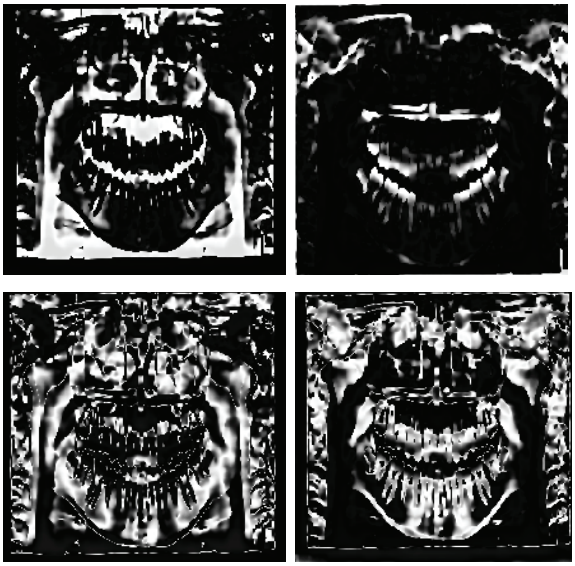

Figure 4 illustrates and simplifies the visual representation by segmentation. Different inputs and their outcomes are illustrated in the above Figures. The FCM technique is used to conduct image segmentation on dental pictures, simplifying and streamlining the classification procedure.

4.3.3. Optimised Score Estimation Ant Lion Optimization (ALO)

The segmented dental images are utilized for generating the optimal score, whereas the ALO is employed in generating the optimal feature values. ALO does the generation of the best or optimal score from the segmented image. The Ant Lion Optimizer (ALO) is a recently published innovative algorithm that replicates the foraging behavior of Ant lions. It has recently been used to solve a large variety of optimization issues. It offers several advantages, including ease of use, scalability, flexibility, and a good

mix between exploration and exploitation. The deep learning and optimization approach simplifies the process and minimizes the complexity. From the ALO, an optimal score of 0.719 is retrieved that is utilized in the training of classifier Deep CNN. The network is trained with the optimized value to acquire the distinct classification.

4.3.4. Classification of Age

With the aid of optimum score selection using the Ant-Lion Optimization (ALO) approach, the preprocessed and segmented dental picture is categorized to determine chronological age. Table 1 and Figure 5 show the DCNN's classification performance.

Table 1
Comparison of age classification

Method	Sensitive (%)	Specificity (%)	Accuracy (%)
Naïve Bayes (NB)	76	79	76
Random Forest (RF)	95.5	86	91
Support Vector Machine (SVM)	85	80.5	83
Convolutional Neural Network (CNN)	75	80	77.5
Deep CNN	100	90	91

Figure 5 compares the effectiveness of age categorization with the proposed DCNN and the current method. The suggested method's classification accuracy is comparable to that of the RF classifier, and DCNN performs better than NB, CNN, and SVM, respectively, by 15%, 13.5%, and 8%. The classification sensitivity of the suggested approach DCNN is greater than RF, NB, CNN, and SVM, respectively, by 4%, 11%, 10%, and 9.5%. The classification specificity of the suggested approach DCNN is greater than that of RF, NB, CNN, and SVM, respectively, by 4.5%, 24%, 25%, and 15%. The suggested DCNN outperforms the current method in terms of classification performance.

Figure 5

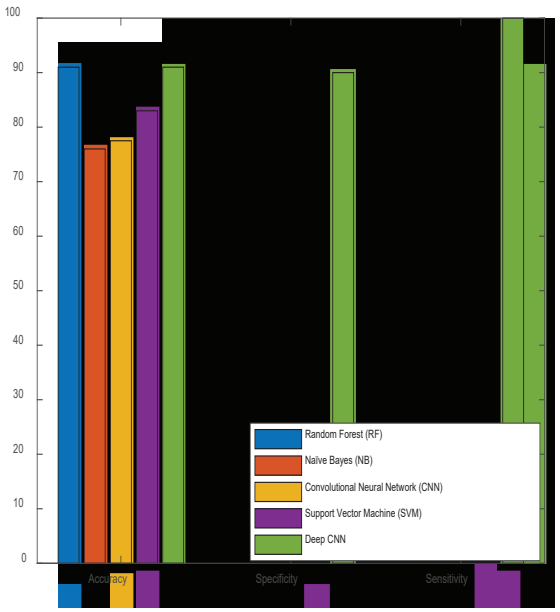

(a) DCNN's classification performance

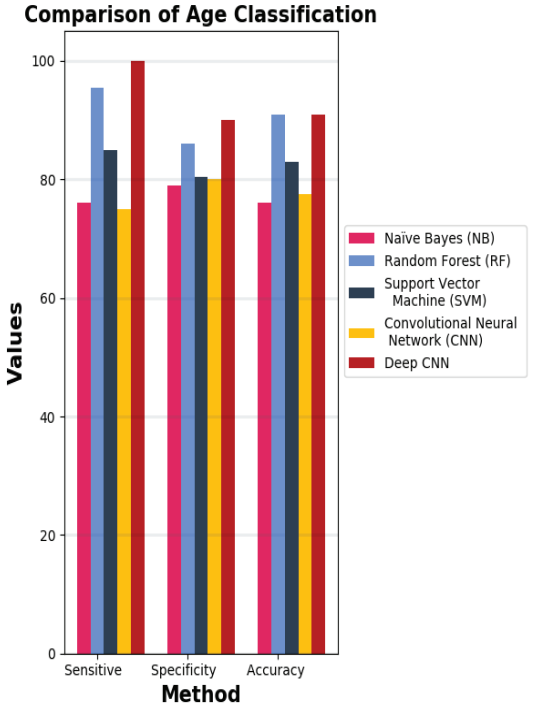

(b) Comparison of Age Classification

4.3.5. Classification of Gender

With the use of optimized score determination and the Ant-Lion Optimization (ALO) approach, the pre-processed and segmented dental picture is classed to determine gender as well as age. 12 photos are taken into account for gender as well as age categorization (5 men and 7 females), and 11 of them are accurately categorized. Geometric characteristics and the best scores produced by the ALO approach are used to classify genders as well as age. Table 2, and Figure 6 provide the DCNN's performance of the classifier.

Table 2

Comparison of gender classification

Method	Sensitivity (%)	Specificity (%)	Accuracy (%)
Naïve Bayes (NB)	75	80	77.5
Random Forest (RF)	95	85	90
Support Vector Machine (SVM)	85	80	82.5
Convolutional Neural Network (CNN)	76	81	78
Deep CNN	100	85.7	91.7

Figure 6 compares the efficiency of the suggested DCNN with the current method for gender categorization. The suggested technique DCNN has a better classification accuracy {1.7%, 14.2%, 13.7%, and 9.2%} than {RF, NB, CNN, and SVM} respectively. The classification sensitivity of the suggested approach DCNN is higher than that of RF, NB, CNN, and SVM, respectively, by 0.7%, 5.7%, 4.7%, and 5.7%. The classification specificity of the suggested approach DCNN is greater than RF, NB, CNN, and SVM, respectively, by 5%, 25%, 24%, and 15%. The suggested DCNN outperforms the current method in terms of classification performance.

The visual representation of DCNN categorization and the forecast summary is shown in Figure 8 along with a confusion matrix that shows the number of correct and incorrect classifications as distinct classes.

Figure 6

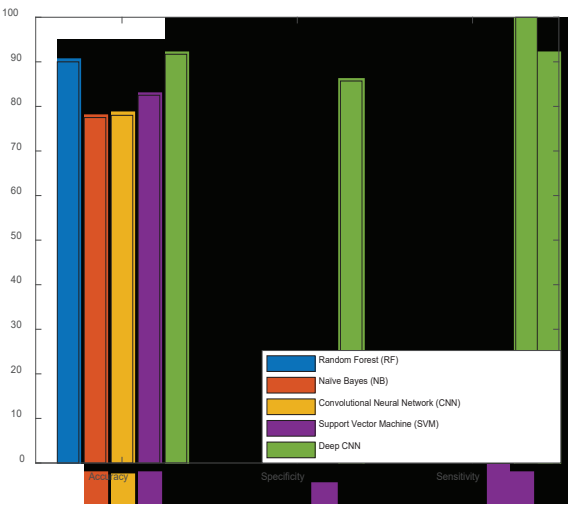

(a) DCNN's classification performance

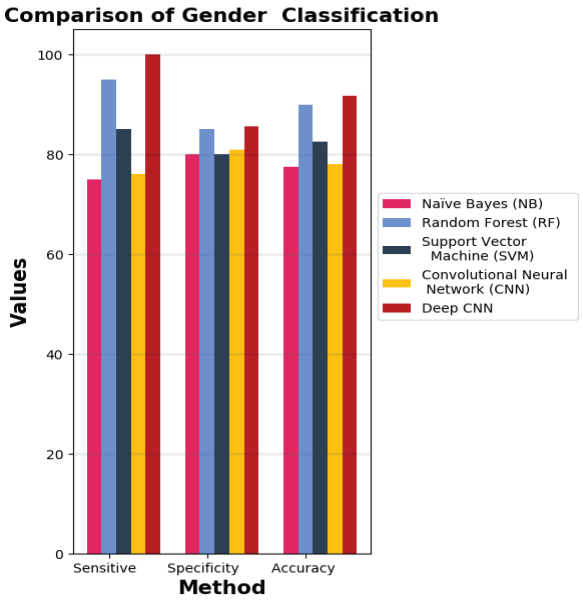

(b) Comparison of Age Classification

In Figure 9, the occurrence of error or loss over the routine of the DCNN and rate accuracy for different iterations is given. The rate of accuracy increases at iteration three, and loss decreases at iteration 2. The performance of the DCNN is enriched with the de-

Figure 7
Confusion Matrix for age classification

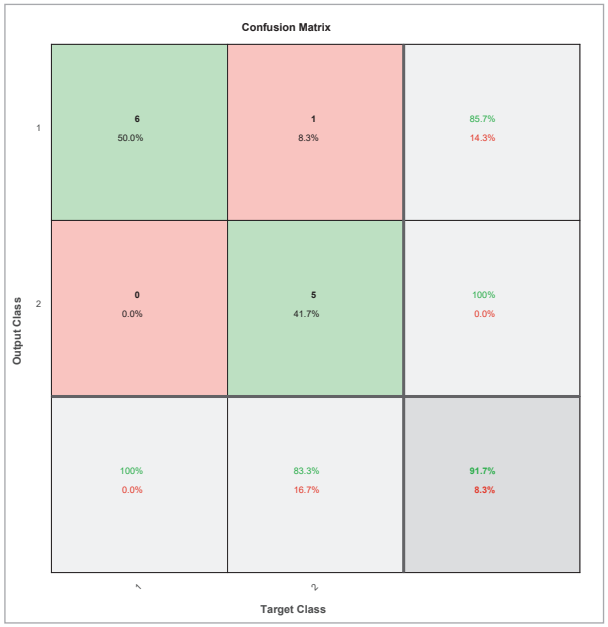

Figure 8
Accuracy and loss functions are compared to iteration

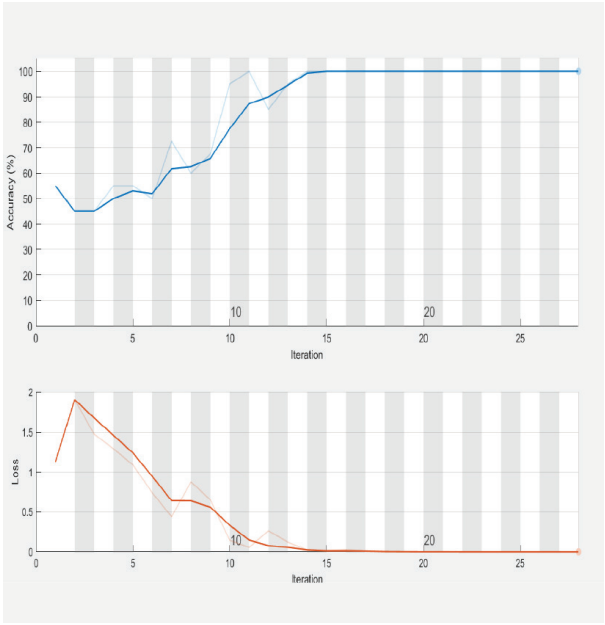

crease of the loss function, whereas a practical classification of age and gender is achieved. Accuracy is utilized in measuring the performance of the classifier, and the loss function optimizes performance. In DCNN, the loss function decreases respectively to increase accuracy and iteration. That is, the classifier model is efficient over increased iteration.

The age and gender classification using other recent methods are given in Table 4. The approaches like FNN-TLBO and Spike neuron-based CNN are compared with the proposed technique. The values in the table are depicted in Figure 9.

The age and gender classification are attained for the two different new approaches with the dataset utilized by the authors [16, 29, 7]. From the observation, it is identified that the proposed approach is more effective than the other two approaches.

Table 3
Comparison of performance

Classification	Method	Sensitive (%)	Specificity (%)	Accuracy (%)
Age Classification	Fuzzy Neural Network with Teaching Learning - Based Optimization (FNN-TLBO)	92	89.12	89
	Spike neuron-based CNN	99.6	100	100
	Deep CNN	91	90	100
Gender Classification	Fuzzy Neural Network with Teaching Learning - Based Optimization (FNN-TLBO)	91	92	90
	Spike neuron-based CNN	93.8	100	88.9
	Deep CNN	91.7	85.7	100

Figure 6

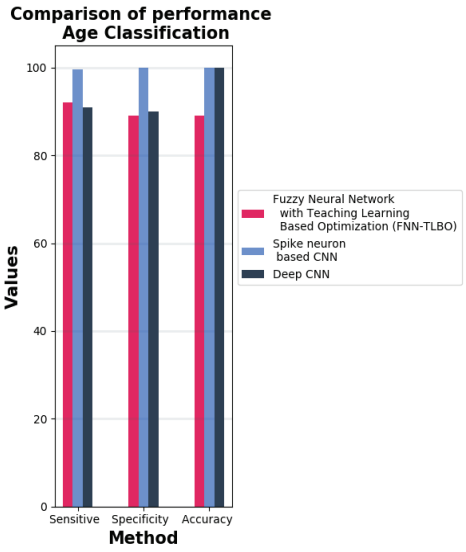

(a) Comparison of Performance – Age Classification

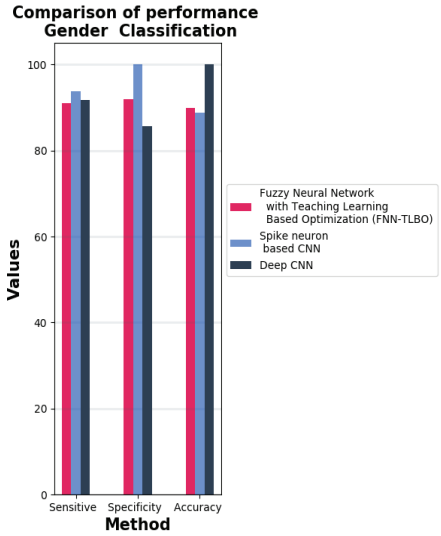

(b) Comparison of Performance – Gender Classification

5. Conclusion

This research performs the dental base age analysis using deep learning models. It further helps experts to identify the age and gender in a short time without any doubts. The primary intent of this research work is to identify the exact gender and age of children or juveniles. The processing methodology of the dental image is a complicated process, and hence, this research work focuses on the processing of the dental image to acquire gender and age. The noise in the OPG image is processed and enhanced by ADF with the HE technique. The process of analyzing and classifying are simplified by the FCM-based segmentation and ALO-based optimal feature score selection, respectively. The needed parts of the teeth are segmented, and the geometric features are retrieved with optimal values. This processed image is passed to the classifier DCNN where the age and gender are classified effectively. The proposed DCNN achieves 91.7% for gender classification and 91% accuracy for age classification. The approach with the maximal image is not investigated and it can be done in the future. The suggested DCNN outperforms the current state-of-the-art approaches when the proposed method's results are compared to them. The limitation of the proposed approach is an occurrence of an error during training that can be improved by some other deep-learning approaches.

References

1. Acharya, A. B., Mainali, S. Sex Discrimination Potential of Buccolingual and Mesiodistal Tooth Dimensions. Journal of Forensic Sciences, 2008, 53(4), 790-792. https://doi.org/10.1111/j.1556-4029.2008.00778.x

2. Agarap, A. F. An Architecture Combines a Convolutional Neural Network (CNN) and Supports Vector Machine (SVM) for Image Classification. arXiv preprint, 2017. arXiv:1712.03541.

3. Akkoç, B., Arslan, A., Kök, H. Automatic Gender Determination from 3D Digital Maxillary Tooth Plaster Models Based on the Random Forest Algorithm and Discrete Cosine Transform. Computer Methods and Programs in Biomedicine, 2017, 143, 59-65. https://doi.org/10.1016/j.cmpb.2017.03.001
4. Akkoç, B., Arslan, A., Kök, H. Grey Level co-Occurrence and Random Forest Algorithm-based Gender Determination with Maxillary Tooth Plaster Images. Computers in Biology and Medicine, 2016, 73, 102-107. https://doi.org/10.1016/j.compbiomed.2016.04.003
5. Alkaabi, S., Yussof, S., Al-Mulla, S. Evaluation of Convolutional Neural Network Based on Dental Images for Age Estimation. In 2019 International Conference on Electrical and Computing Technologies and Applications (ICECTA), 2019, 1-5. https://doi.org/10.1109/ICECTA48151.2019.8959665
6. Avuçlu, E., Başçiftçi, F. Determination Age and Gender with Developed a Novel Algorithm in Image Processing Techniques by Implementing Dental X-Ray Images. Romanian Journal of Legal Medicine, 2018, 26(4), 412-418.
7. Balan, H., Alrasheedi, A. F., Askar, S. S., Abouhawwash, M. An Intelligent Human Age and Gender Forecasting Framework Using Deep Learning Algorithms. Applied Artificial Intelligence, 2022, 36(1). https://doi.org/10.1080/08839514.2022.2073724
8. Braga, J., Heuze, Y., Chabadel, O., Sonan, N. K., Gueramy, A. Non-Adult Dental Age Assessment: Correspondence Analysis and Linear Regression versus Bayesian Predictions. International Journal of Legal Medicine, 2005, 119(5), 260-274. https://doi.org/10.1007/s00414-004-0494-8
9. Chuang, K. S., Tzeng, H. L., Chen, S., Wu, J., Chen, T. J. Fuzzy C-Means Clustering with Spatial Information for Image Segmentation. Computerized Medical Imaging and Graphics, 2006, 30(1), 9-15. https://doi.org/10.1016/j.compmedimag.2005.10.001
10. Connor, R., Cardillo, F. A. Quantifying the Specificity of Near-Duplicate Image Classification Functions. In 11th International Joint Conference on Computer Vision, Imaging and Computer Graphics Theory and Applications. 2016. https://doi.org/10.5220/0005785406470654
11. Damaševičius, R., Seda, C., Gokhan, S., Sanjay, M., Rytis, M. Gender Detection Using 3D Anthropometric Measurements by Kinect. Metrology and Measurement Systems, 2018, 25(2).
12. Esmaeilyfard, R., Paknahad, M., Dokohaki, S. Sex Classification of First Molar Teeth in Cone-Beam Computed Tomography Images Using Data Mining. Forensic Science International, 2021, 318, 110633. https://doi.org/10.1016/j.forsciint.2020.110633
13. Foody, G. M. Harshness in Image Classification Accuracy Assessment. International Journal of Remote Sensing, 2008, 29(11), 3137-3158. https://doi.org/10.1080/01431160701442120
14. Galibourg, A., Cussat-Blanc, S., Dumoncel, J., Telmon, N., Monsarrat, P., Maret, D. Comparison of Different Machine Learning Approaches to Predict Dental Age Using Demirjian's Staging Approach. International Journal of Legal Medicine, 2021, 135(2), 665-675. https://doi.org/10.1007/s00414-020-02489-5
15. Hemalatha, B., Rajkumar, N. A Modified Machine Learning Classification for Dental Age Assessment with Effectual ACM-JO-based Segmentation. International Journal of Bio-Inspired Computation, 2021, 17(2), 95-104. https://doi.org/10.1504/IJBIC.2021.114089
16. Hemalatha, B., Rajkumar, N. A Versatile Approach for Dental Age Estimation Using a Fuzzy Neural Network with Teaching Learning-based Optimization Classification. Multimedia Tools Applied, 2020, 79, 3645-3665. https://doi.org/10.1007/s11042-018-6434-2
17. Houssein, E. H., Mualla, N., Hassan, M. R. Dental Age Estimation based on X-Ray Images. Computers, Materials & Continua, 2020, 62(2), 591-605. https://doi.org/10.32604/cmc.2020.08580
18. Jeyaraj, P. R., Nadar, E. R. S. Computer-Assisted Medical Image Classification for early Diagnosis of Oral Cancer Employing Deep Learning Algorithm. Journal of Cancer Research and Clinical Oncology, 2019, 145(4), 829-837. https://doi.org/10.1007/s00432-018-02834-7
19. Keshtkar, F., Gueaieb, W. Segmentation of Dental Radiographs Using a Swarm Intelligence Approach. In 2006 Canadian Conference on Electrical and Computer Engineering, 2006, 328-331. https://doi.org/10.1109/CCECE.2006.277656
20. Lai, Y. H., Lin, P. L. Effective Segmentation for Dental X-Ray Images Using Texture-based Fuzzy Inference System. In International Conference on Advanced Concepts for Intelligent Vision Systems, Springer, Berlin, Heidelberg, 2008, 936-947. https://doi.org/10.1007/978-3-540-88458-3_85
21. Lin, P. L., Lai, Y. H., Huang, P. W. A Practical Classification and Numbering System for Dental Bitewing Radiographs Using Teeth Region and Contour Information. Pattern Recognition, 2010, 43(4), 1380-1392. https://doi.org/10.1016/j.patcog.2009.10.005

22. Mirjalili, S. The Ant Lion Optimizer. Advances in Engineering Software, 2015, 83, 80-98. https://doi.org/10.1016/j.advengsoft.2015.01.010

23. Narkhede, S. Understanding Auc-roc Curve. Towards Data Science, 2018, 26, 220-227.

24. Pandey, P., Bhan, A., Dutta, M. K., Travieso, C. M. Automatic Image Processing Based on Dental Image Analysis Using Automatic Gaussian Fitting Energy and Level Sets. In 2017 International Conference and Workshop on Bioinspired Intelligence, 2017, 1-5. https://doi.org/10.1109/IWOBI.2017.7985529

25. Paul, A., Mukherjee, D. P., Das, P., Gangopadhyay, A., Chintha, A. R., Kundu, S. Improved Random Forest for Classification. IEEE Transactions on Image Processing, 2018, 27(8), 4012-4024. https://doi.org/10.1109/TIP.2018.2834830

26. Senthilkumaran, N., Thimmiaraja, J. Histogram Equalization for Image Enhancement using MRI Brain Images. In 2014 World Congress on Computing and Communication Technologies, 2014, 80-83. https://doi.org/10.1109/WCCCT.2014.45

27. Sultana, F., Sufian, A., Dutta, P. Advancements in Image Classification Using a Convolutional Neural Network. In 2018 Fourth International Conference on Research in Computational Intelligence and Communication Networks (ICRCICN), 2018, 122-129. https://doi.org/10.1109/ICRCICN.2018.8718718

28. Tuan, T. M., Fujita, H., Dey, N., Ashour, A. S., Ngoc, V. T. N., Chu, D. T. Dental Diagnosis from X-Ray Images: An Expert System Based on Fuzzy Computing. Biomedical Signal Processing and Control, 2018, 39, 64-73. https://doi.org/10.1016/j.bspc.2017.07.005

29. Viji, C., Beschi, Raja J., Parthasarathi, P., Ponmagal, R.S. Efficient Fuzzy based k-Nearest Neighbor Technique for Web Services Classification. Microprocessors and Microsystems, 2020, 76(103097), 1274-1278. https://doi.org/10.1016/j.micpro.2020.103097

30. Vila-Blanco, N., Carreira, M. J., Varas-Quintana, P., Balsa-Castro, C., Tomas, I. Deep Neural Networks for Chronological Age Estimation from OPG Images. IEEE Transactions on Medical Imaging, 2020, 39(7), 2374-2384. https://doi.org/10.1109/TMI.2020.2968765

31. Weickert, J. Anisotropic Diffusion in Image Processing, 1998, 1, 59-60.

32. Wolf, T. G., Briseño-Marroquín, B., Callaway, A., Patyna, M., Müller, V. T., Willershausen, I., Willershausen, B. Dental Age Assessment in 6-to 14-year old German Children: Comparison of Cameriere and Demirjian Methods. BMC Oral Health, 2016, 16(1), 1-8. https://doi.org/10.1186/s12903-016-0315-8

33. Wolfart, S., Menzel, H., Kern, M. Inability to Relate Tooth Forms to Face Shape and Gender. European Journal of Oral Sciences, 2004, 112(6), 471-476. https://doi.org/10.1111/j.1600-0722.2004.00170.x

34. Wu, J., Pan, S., Zhu, X., Cai, Z., Zhang, P., Zhang, C. Self-Adaptive Attribute Weighting for Naive Bayes Classification. Expert Systems with Applications, 2015, 42(3), 1487-1502. https://doi.org/10.1016/j.eswa.2014.09.019

35. Yan, L. C., Yoshua, B., Geoffrey, H. Deep Learning. Nature, 2015, 521(7553), 436-444. https://doi.org/10.1038/nature14539